

Journal of Materials Chemistry C

Accepted Manuscript



This is an *Accepted Manuscript*, which has been through the Royal Society of Chemistry peer review process and has been accepted for publication.

Accepted Manuscripts are published online shortly after acceptance, before technical editing, formatting and proof reading. Using this free service, authors can make their results available to the community, in citable form, before we publish the edited article. We will replace this *Accepted Manuscript* with the edited and formatted *Advance Article* as soon as it is available.

You can find more information about *Accepted Manuscripts* in the [Information for Authors](#).

Please note that technical editing may introduce minor changes to the text and/or graphics, which may alter content. The journal's standard [Terms & Conditions](#) and the [Ethical guidelines](#) still apply. In no event shall the Royal Society of Chemistry be held responsible for any errors or omissions in this *Accepted Manuscript* or any consequences arising from the use of any information it contains.

Effect of cyano group on solid state photophysical behavior of tetraphenylethene substituted benzothiadiazoles

Thaksen Jadhav, Bhausahab Dhokale, Rajneesh Misra*

Department of Chemistry, Indian Institute of Technology Indore,
Madhya Pradesh, 452 017, India.

*E-mail: rajneeshmisra@iiti.ac.in; Fax: +91 731 2361 482; Tel: +91 731 2438 710.

Abstract

Two unsymmetrical tetraphenylethene (TPE) substituted Donor-Acceptor (D-A) benzothiadiazoles (BTDs) **3a**, and **3b** were designed and synthesized by the Suzuki cross-coupling reaction. The design strategy was opted to maintain the donor (TPE) fragment constant and the acceptor strength of BTD was modulated by using phenyl and cyanophenyl units. Their solvatochromism, aggregation induced emission (AIE) and mechanochromic properties were investigated. The BTDs **3a**, and **3b** exhibit strong solvatochromic and AIE behavior. The cyano-group containing BTD **3b** exhibits reversible mechanochromic behavior with high color contrast between green and yellow, whereas **3a** do not show mechanochromism. The solid state absorption and emission properties of BTDs **3a**, and **3b** show different behavior in their pristine and ground form. The powder XRD study shows reversible morphological change between crystalline and amorphous phase upon grinding.

Introduction

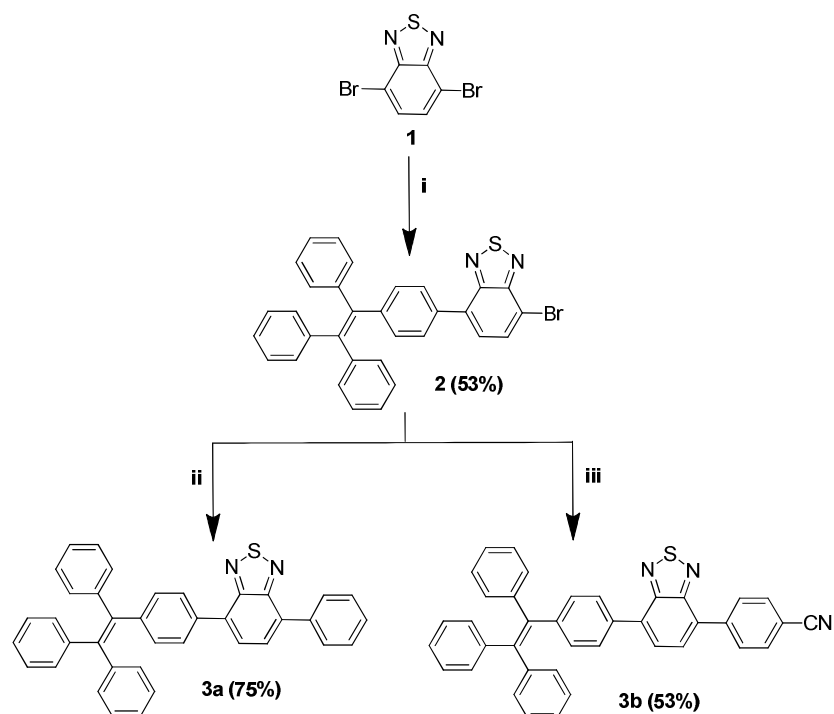
The design of organic molecular systems exhibiting aggregation induced emission (AIE) and mechanochromic properties has gained considerable attention due to their potential applications

in the field of mechano-sensors, optical recording, security papers and optoelectronic devices.¹ Solid state emission with high color contrast is an essential criteria for mechanochromism.² The conventional organic molecules are non-emissive in solid state due to the notorious aggregation caused quenching (ACQ) effect.³ The exactly opposite phenomenon to ACQ was introduced by Tang *et al*, which is called aggregation induced emission (AIE).⁴ The tetraphenylethylene (TPE) is propeller shaped AIE active unit and has been explored for design of environmental stimuli responsive mechanochromic materials.⁵

Generally the donor-acceptor (D-A) type molecular systems show low fluorescence quantum efficiency in solution as well as in the solid state. 2,1,3-Benzothiadiazole (BTD) is a strong acceptor owing to its electron deficient nature.⁶ Wang *et al* and Wei *et al* had reported symmetrical benzothiadiazole based cyano-substituted diphenylethene derivatives for mechanochromic properties and studied the effect of D-A strength on their mechanochromism.⁷ The literature reveals, there are no reports on the mechanochromic behavior of TPE substituted BTDs.⁸ Our group is involved in the design and synthesis of TPE substituted mechanochromic materials.⁹ We have explored symmetrical and unsymmetrical BTDs for photonic applications.¹⁰ In a recent contribution, we have shown dipyrindylamine substituted unsymmetrical BTD for mechanochromism.¹¹ Herein we have designed and synthesized TPE substituted unsymmetrical D-A benzothiadiazoles (BTDs) **3a**, and **3b** and studied their photophysical and mechanochromic properties. The design of the TPE substituted unsymmetrical BTDs are based on the following considerations: (1) The use of TPE as donor unit as well as AIE activator. The TPE moiety offers the solid with large free volume and intramolecular rotations. (2) The acceptor strength of BTD is altered by using phenyl as weak donor in **3a** and 4-cyanophenyl as weak acceptor in **3b** by keeping TPE as donor (D) on one side of BTD. (3) The cyano-group is used to increase the

acceptor strength of BTD, and also as source for hydrogen bonding.^{9a,12} Thus the combination of TPE, BTD and cyano group will provide the place to change the D-A effect. The results show BTD **3b** exhibits reversible mechanochromic behavior with color contrast between green and yellow.

Results and discussions



Scheme 1. Synthetic route for the BTDs **3a** and **3b**.

(i) 4-(1,2,2-triphenylvinyl)phenylboronic acid pinacol ester, K_2CO_3 , $Pd(PPh_3)_4$, Toluene:Ethanol:Water; (ii) phenylboronic acid, K_2CO_3 , $Pd(PPh_3)_4$, Toluene:Ethanol:Water; (iii) 4-cyanophenylboronic acid pinacol ester, K_2CO_3 , $Pd(PPh_3)_4$, Toluene:Ethanol:Water.

The TPE substituted bromo-BTD intermediate **2** was synthesized by the Pd-catalyzed Suzuki cross-coupling reaction of the dibromo-BTD **1**, with the 4-(1,2,2-triphenylvinyl)phenylboronic acid pinacol ester (0.9 equivalent) in 53% yield (Scheme 1). The Suzuki cross-coupling reaction of TPE substituted bromo-BTD **2** with phenylboronic acid and 4-cyanophenylboronic acid

pinacol ester in presence of $\text{Pd}(\text{PPh}_3)_4$ as catalyst resulted unsymmetrical TPE substituted BTDs **3a**, and **3b** in 75% and 55% yield respectively. The 4-(1,2,2-triphenylvinyl)phenylboronic acid pinacol ester was synthesized by using reported procedure. The TPE substituted BTDs **3a**, and **3b** were well characterized by ^1H NMR, ^{13}C NMR and HRMS techniques. The ^1H NMR spectra of **3b** show downfield shift of protons of BTD unit and phenyl rings attached to BTD unit compared to **3a**. This reveals that the electron withdrawing effect of cyano-group reduces the electron density on BTD unit and makes BTD unit stronger acceptor. Thermo gravimetric analysis (TGA) of unsymmetrical BTDs **3a** and **3b** reveals good thermal stability. The thermal decomposition temperatures (T_d) corresponding to 5% weight loss under nitrogen atmosphere was observed at 357 $^\circ\text{C}$, and 280 $^\circ\text{C}$ for **3a** and **3b** respectively (Fig. S1).

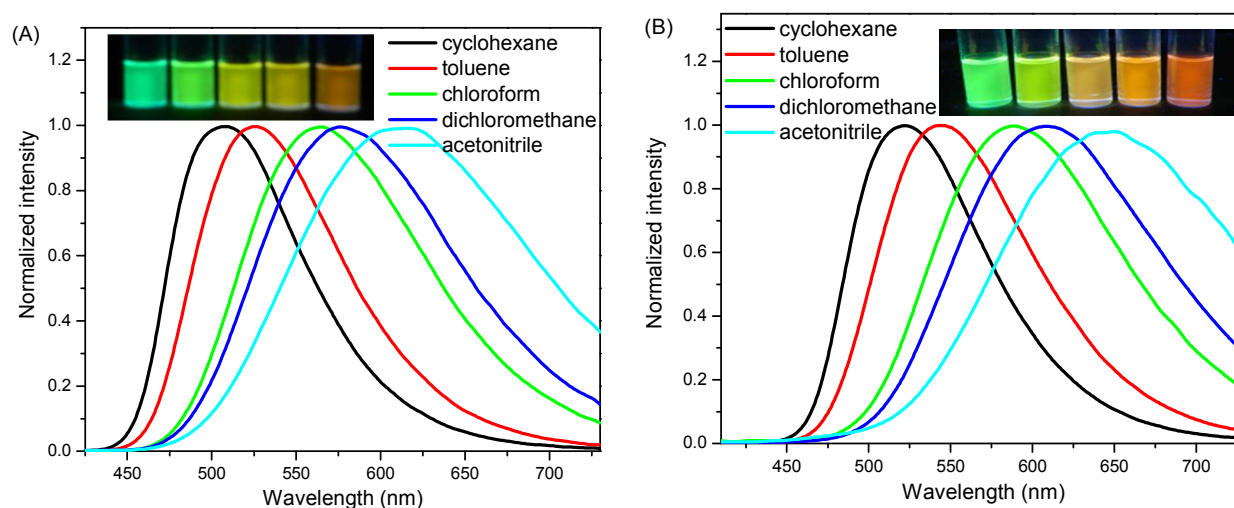


Fig. 1 Photoluminescence spectra of **3a** (A) and **3b** (B) in different solvents with varying polarities (concentration of luminogens = 1×10^{-5} M, excitation wavelength or λ_{ex} = 370 nm). The insets of (A) and (B) show luminescence photographs of **3a** and **3b** in cyclohexane, toluene, chloroform, dichloromethane, acetonitrile (from left to right) under 365 nm illumination

The absorption and fluorescence spectra of BTDs **3a** and **3b** were recorded in tetrahydrofuran solution and corresponding data are listed in Table S1. The BTDs **3a** and **3b** exhibit a strong absorption band between 250–350 nm corresponding to $\pi \rightarrow \pi^*$ transition and a charge transfer (CT) band from TPE to BTD unit between 360–460 nm.¹⁰ Generally, the TPE containing fluorophores are poorly emissive in solution, due to loss of excited state energy by intramolecular rotations of TPE, but the BTDs **3a** and **3b** were highly emissive.³ The BTDs **3a** and **3b** upon excitation show strong yellow green (λ :555 nm) and yellow (λ :588 nm) emission respectively. The effect of solvent polarity on the absorption and emission was investigated. The CT absorption band of BTDs **3a** and **3b** exhibits slight blue shift with increase in solvent polarity (Table S1). The fluorescence spectra show large red shift as the solvent was changed from cyclohexane for **3a** (λ :509 nm) and **3b** (λ :523 nm) to acetonitrile **3a** (λ :614 nm) and **3b** (λ :649 nm). The fluorescence quantum yield was decreased by changing the solvent polarity from nonpolar to polar (Table S1). This shows that the charge separation and dipole moment in the excited state is larger than in the ground state. The solvent dependence on absorption and emission was confirmed by the Lippert-Mataga plot, which shows a linear correlation of the Stokes shift with solvent polarity (Fig. S3 and S4). In all the solvents BTD **3b** show red shifted emission than BTD **3a** indicating better D-A nature.

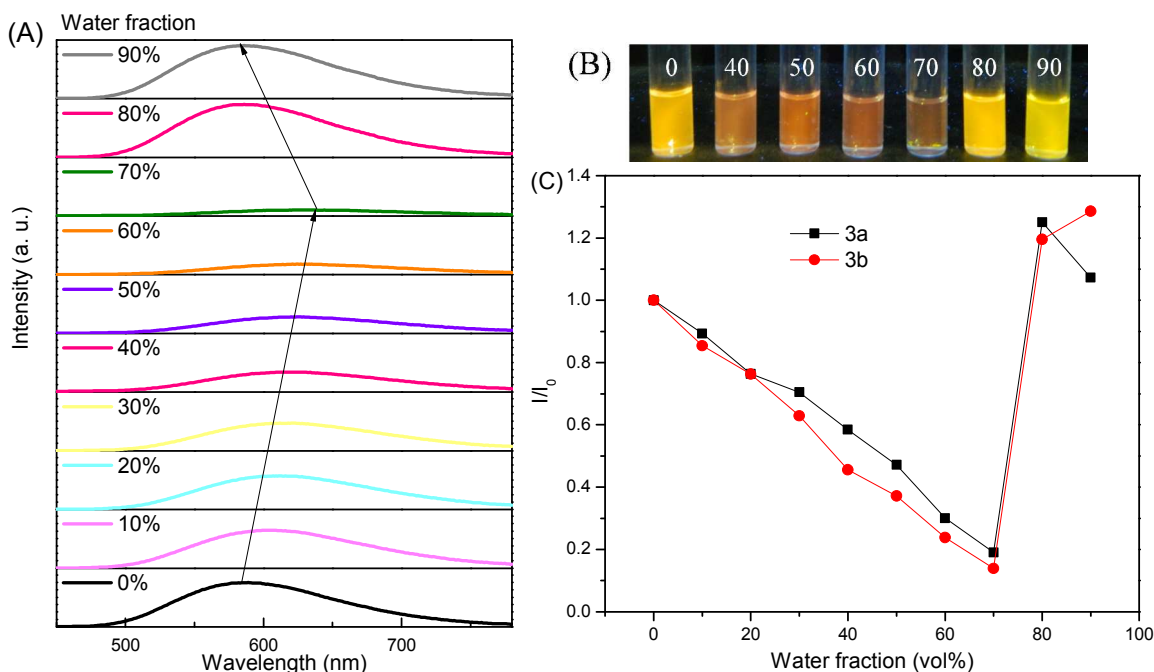


Fig. 2 Fluorescence spectra of **3b** (A) in THF-water mixtures with different water fractions (f_w). (B) Fluorescence photographs of **3b** in THF-water mixtures with different water fractions under 365 nm UV illumination. (C) Plot of fluorescence intensity vs. f_w . Luminogen concentration: 10 μ M; excitation wavelength: 400 nm; intensity at λ_{max} .

The AIE property of the unsymmetrical BTDs **3a** and **3b** were studied with the help of absorption and fluorescence spectroscopy. The BTDs **3a** and **3b** are highly soluble in the tetrahydrofuran (THF) and sparingly soluble in water. The nanoaggregates of BTDs **3a** and **3b** were prepared by increasing the percentage of water in THF solution. In pure THF solution, BTD **3a** show bright yellowish green luminescence (λ :555 nm), whereas BTD **3b** show bright yellow luminescence (λ :588 nm). By increasing the water fraction (f_w) upto 70% (f_w), a gradual red shift of 32 nm for **3a** (λ :587 nm) and 46 nm for **3b** (λ :634 nm) with decrease in the fluorescence intensity was observed (Fig. 2 and Fig. S5). This can be attributed to the increased polarity of solvent and stabilization of charge-transfer state.¹³ The large red shift at 70% (f_w) in **3b** compared to **3a** also indicates strong D-A interaction in **3b** compared to **3a**. Beyond 70% (f_w)

once again fluorescence intensity was increased with blue shifted emission. The BTD **3a** show bright yellowish green luminescence (λ :540 nm) and BTD **3b** emits bright yellow luminescence (λ :574 nm) at 90% (f_w) (Fig. 2b and S6). This increase in the fluorescence intensity was attributed to the AIE phenomenon, here AIE is dominating the effect of solvent polarity.

The mechanochromic properties of BTDs **3a** and **3b** were explored by emission studies. The pristine solid of BTDs **3a** and **3b** show green emission at 521 nm and 526 nm respectively. The BTD **3b** upon grinding by a spatula or pestle converts the green emitting solid to yellow emitting solid. The ground form of BTD **3b** shows emission peak \sim 565 nm with red shift of 44 nm, whereas no color change was observed for **3a** (Fig. 3). The pristine form and ground form of BTD **3a** emits at \sim 526 nm. The mechanochromic effect in BTD **3b** is highly reversible and can be reverted to its original color by annealing at 80 °C for 5 min, indicating excellent reversibility of the BTD (Fig. S9). The regeneration to pristine form can also be achieved by fuming with dichloromethane vapor for 2 min, but the reproducibility was poor through fumigation and emissions at different wavelengths were observed. In order to understand the mechanochromic behavior of BTDs **3a** and **3b**, solid state absorption studies were performed. The synthesized solids of **3a** and **3b** absorb at 485 nm and 476 nm respectively (Fig. S7). Upon grinding **3a** absorbs at 466 nm, whereas **3b** absorbs at 492 nm. This small change in absorption spectra of **3b** with color change from greenish yellow to yellow can be visualized by naked eye, while no color change was observed for **3a** (Fig. S8).

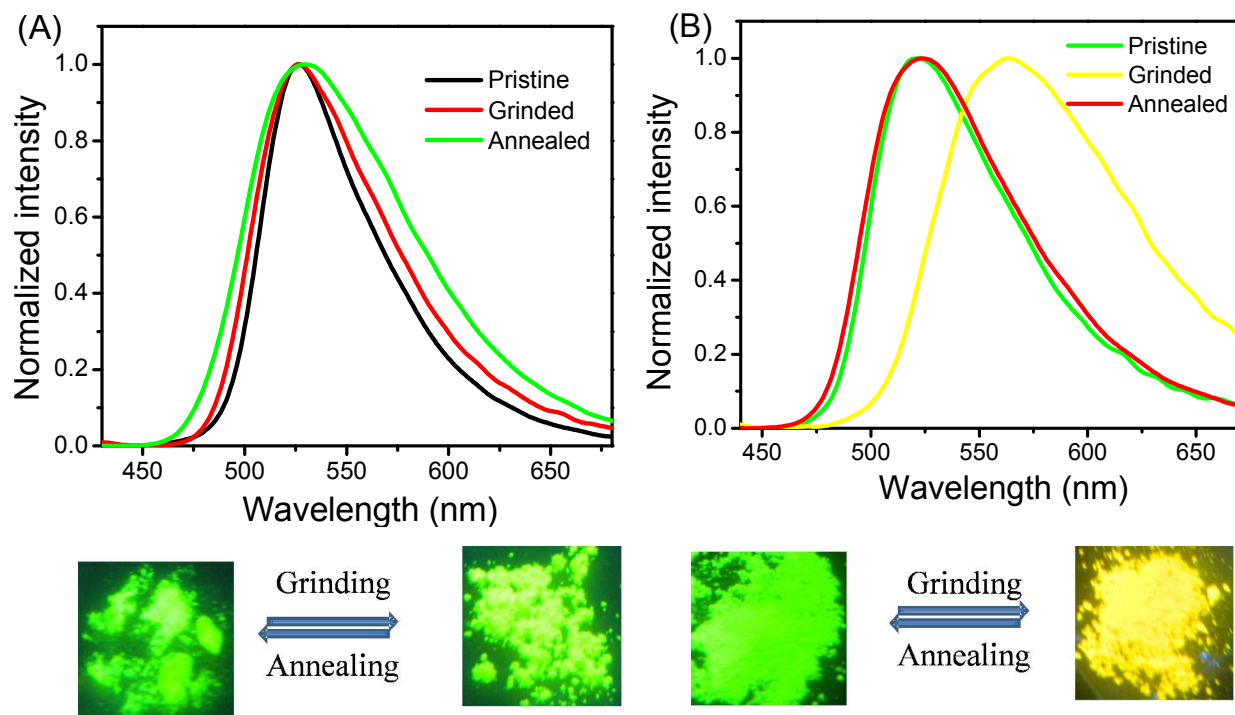


Fig. 3 Emission spectra of **3a** (A) and **3b** (B) as pristine, ground and annealed solids and photograph taken under 365 nm UV illumination.

The comparison of photophysical properties in solution and solid state reflects the strength of D-A interaction. The absorption and emission spectra in solution and solid state show: (i) In all the solvents, **3b** show red shifted absorption and emission compared to **3a** indicating strong D-A interaction in **3b** (Table S1). (ii) The pristine form of **3b** shows blue shifted absorption than **3a** and emits at similar region suggesting weak D-A interaction in pristine form, which is contrary with results in solution state. This may be due to different solid state packing and twisting in molecular backbone. (iii) After grinding **3b** shows red shift in both absorption and emission,

whereas **3a** shows blue shifted absorption and similar emission. This reveals that upon grinding **3a** shows decreased D-A interaction, whereas **3b** shows enhanced D-A interaction.

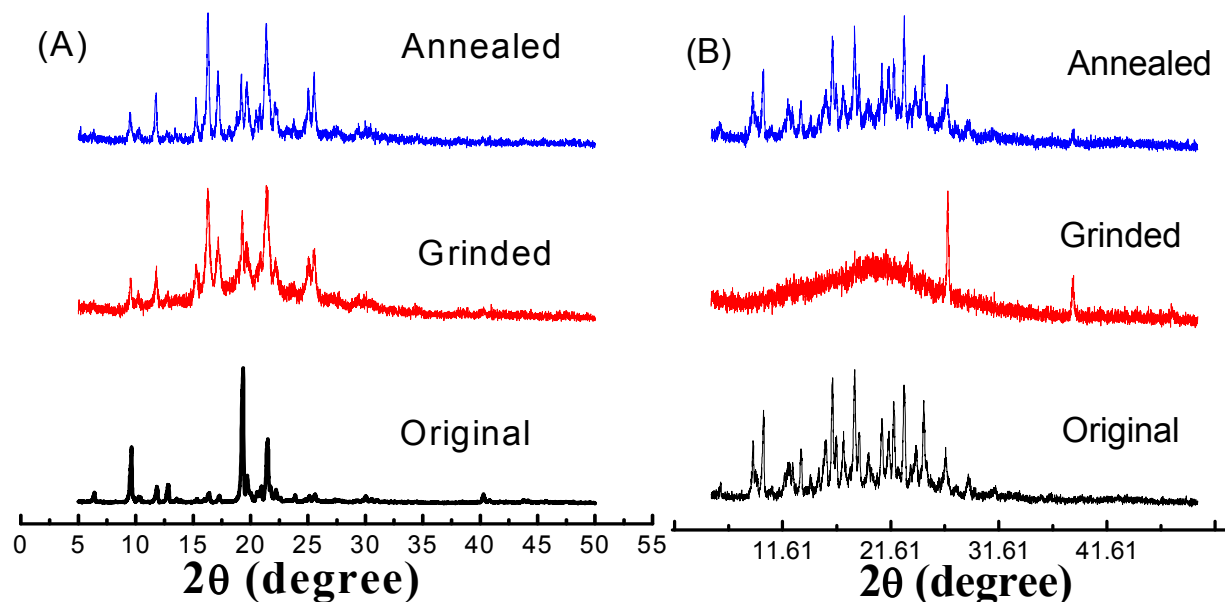


Fig. 4 Powder XRD patterns of BTDs **3a** and **3b** in the state of as-prepared solid, after grinding and annealing treatment.

The powder X-ray diffraction (PXRD) analysis was performed for BTDs **3a** and **3b** in pristine, ground and annealed forms (Fig. 4). The BTDs **3a** and **3b** exhibit sharp diffraction peaks before grinding, reflecting the crystalline character. Upon grinding BTD **3b**, the sharp diffraction peaks disappeared and a diffused band was generated indicating the transition from crystalline to amorphous state. The ground sample of **3b** when subjected to annealing or fumigation, the sharp diffraction peaks were observed indicating the regeneration of crystalline form. In case of **3a** the grinding generates new peaks in PXRD, indicating conversion from one crystalline form to another. The PXRD studies clearly suggest that the mechanochromism in BTD **3b** is associated with the morphology change from the crystalline state to the amorphous state and *vice versa*.

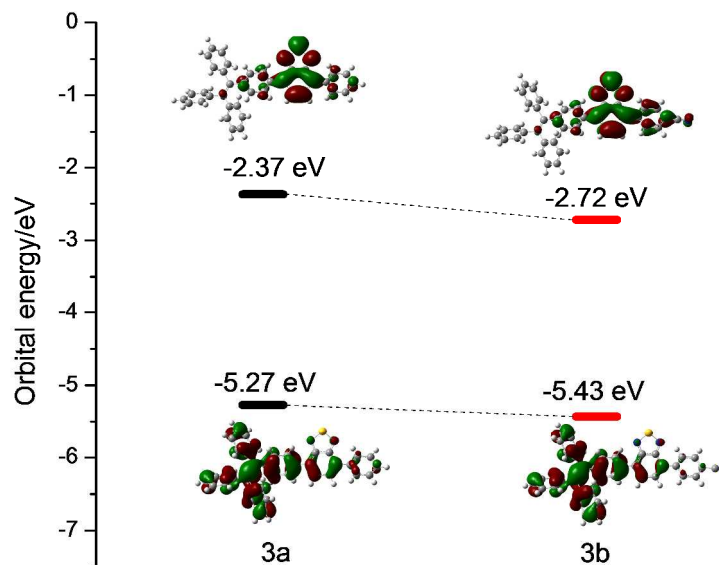


Fig. 5 Correlation diagram showing the HOMO, and LUMO wave functions and energies of the BTDs **3a** (left) and **3b** (right), as determined at the B3LYP/6-31G(d) level.

To gain insight into the electronic structures of the BTDs **3a** and **3b**, density functional theory (DFT) calculation was performed at the B3LYP/6-31G(d) level. The contours of the HOMO and LUMO of BTDs **3a** and **3b** are shown in Fig. 5. The HOMO orbitals are localized over TPE, and benzo part of the BTD unit, whereas the LUMO orbitals are localized on the BTD and phenyl or cyano-phenyl unit. The incorporation of cyano group on the phenyl unit leads to stabilization of both the HOMO and LUMO. The extent of stabilization of LUMO is more pronounced compared to HOMO, which leads to low HOMO-LUMO gap in **3b** compare to **3a**. This also supports the stronger D-A interaction in **3b** compared to **3a** in solution state.

Conclusion

In conclusion, we have designed and synthesized two unsymmetrical TPE substituted BTDs **3a** and **3b**. The BTDs **3a** and **3b** exhibit strong solvatochromism with emission ranging from 510 nm to 650 nm. The AIE study reveals that, by increasing water fraction (f_w) upto 70% the solvent polarity influences the emission, whereas above 70% (f_w) the AIE dominate the effect of solvent polarity. The solvatochromic, AIE and computational studies reveal that the TPE substituted unsymmetrical BTD **3b** exhibits strong donor-acceptor interaction compared to **3a**. The BTD **3b** shows reversible high color contrast mechanochromism between green and yellow. The photophysical properties in solid state reveal varying strength of D-A interaction in pristine and ground form, which may be responsible for different mechanochromic behavior in BTDs **3a** and **3b**. The powder XRD results suggest the destruction of solid state packing from crystalline to amorphous state is associated with mechanochromism. The study reveals that the phenyl and cyano phenyl groups are modulating the acceptor strength of BTD. The use of TPE and incorporation of cyano-group plays important role in mechanochromism. The results obtained in this study will help in design of new mechanosensors.

Experimental section

General methods

Chemicals were used as received unless otherwise indicated. All oxygen or moisture sensitive reactions were performed under nitrogen/argon atmosphere. ^1H NMR (400 MHz), and ^{13}C NMR (100MHz) spectra were recorded on on the Bruker Avance (III) 400 MHz instrument by using CDCl_3 . ^1H NMR chemical shifts are reported in parts per million (ppm) relative to the solvent

residual peak (CDCl₃, 7.26 ppm). Multiplicities are given as: s (singlet), d (doublet), t (triplet), q (quartet), dd (doublet of doublets), dt (doublet of triplets), m (multiplet), and the coupling constants, *J*, are given in Hz. ¹³C NMR chemical shifts are reported relative to the solvent residual peak (CDCl₃, 77.36 ppm). Thermogravimetric analyses were performed on the Mettler Toledo Thermal Analysis system. UV-visible absorption spectra were recorded on a Carry-100 Bio UV-visible Spectrophotometer. Emission spectra were taken in a fluoromax-4p fluorimeter from HoribaYovin (model: FM-100). The excitation and emission slits were 2/2 nm for the emission measurements. All of the measurements were done at 25°C. HRMS was recorded on Bruker-Daltonics, micrOTOF-Q II mass spectrometer. The density functional theory (DFT) calculation were carried out at the B3LYP/6-31G(d) level in the Gaussian 09 program.

Synthesis and characterization of intermediate 2:

2: Pd(PPh₃)₄ (0.01 mmol) was added to a well degassed solution of dibromo-BTD (**1**) (0.2 mmol), 4-(1,2,2-triphenylvinyl)phenylboronic acid pinacol ester (0.2 mmol), K₂CO₃ (0.8 mmol) in a mixture of toluene (32 mL)/ ethanol (4.0 mL)/ H₂O (4.0 mL). The resulting mixture was stirred at 80 °C for 24 h under argon atmosphere. After cooling, the mixture was evaporated to dryness and the residue subjected to column chromatography on silica (Hexane-DCM 60:40 in vol.) to yield the desired product **2** as yellow powder. Yield: 53.0 %. ¹H NMR (400 MHz, CDCl₃, 20 °C): δ 7.88 (d, 1H, *J*= 8 Hz), 7.70 (d, 1H, *J*= 8 Hz), 7.55 (d, 1H, *J*= 8 Hz), 7.03-7.19 (m, 17H) ppm; ¹³C NMR (100 MHz, CDCl₃, 20 °C): δ 153.9, 153.0, 144.2, 143.6, 143.5, 143.5, 141.6, 140.3, 134.4, 133.5, 132.2, 131.7, 131.4, 131.3, 131.3, 128.3, 128.0, 127.8, 127.7, 127.6, 126.6, 126.5, 126.5, 112.8, 0.0 ppm; HRMS (ESI): calcd. for C₃₂H₂₁BrN₂S: 545.0682 (M+H)⁺, found 545.0653.

Synthesis and Characterization of 3a and 3b:

3a: Pd(PPh₃)₄ (0.005 mmol) was added to a well degassed solution of **2** (0.1 mmol), phenylboronic acid (0.12 mmol), K₂CO₃ (0.4 mmol) in a mixture of toluene (20 mL)/ ethanol (4.0 mL)/ H₂O (4.0 mL). The resulting mixture was stirred at 80 °C for 24 h under argon atmosphere. After cooling, the mixture was evaporated to dryness and the residue subjected to column chromatography on silica (Hexane-DCM 50:50 in vol.) to yield the desired product **3a** as greenish yellow powder. Yield: 75.0 %. ¹H NMR (400 MHz, CDCl₃, 20 °C): δ 7.95 (d, 2H, *J*= 8 Hz), 7.74-7.79 (m, 4H), 7.55 (t, 2H, *J*=8 Hz), 7.46 (t, 1H, *J*=8 Hz), 7.05-7.21 (m, 17H) ppm; ¹³C NMR (100 MHz, CDCl₃, 20 °C): δ 154.2, 153.9, 143.8, 143.7, 143.6, 143.6, 141.5, 140.5, 137.4, 135.2, 133.1, 132.8, 131.6, 131.5, 131.4, 131.3, 129.2, 128.6, 128.4, 128.3, 128.1, 127.9, 127.8, 127.7, 127.6, 126.6, 126.5, 126.5, 0.0 ppm; HRMS (ESI): calcd. for C₃₈H₂₆N₂S: 565.1733 (M+H)⁺, found 565.1709.

3b: Pd(PPh₃)₄ (0.005 mmol) was added to a well degassed solution of **2** (0.1 mmol), 4-cyanophenylboronic acid pinacol ester (0.12 mmol), K₂CO₃ (0.4 mmol) in a mixture of toluene (20 mL)/ ethanol (4.0 mL)/ H₂O (4.0 mL). The resulting mixture was stirred at 80 °C for 24 h under argon atmosphere. After cooling, the mixture was evaporated to dryness and the residue subjected to column chromatography on silica (Hexane-DCM 50:50 in vol.) to yield the desired product **3b** as greenish yellow powder. Yield: 55.0 %. ¹H NMR (400 MHz, CDCl₃, 20 °C): δ 8.10 (d, 2H, *J*= 8 Hz), 7.77-7.84 (m, 6H), 7.21 (d, 2H, *J*= 8 Hz), 7.05-7.13 (m, 15H) ppm; ¹³C NMR (100 MHz, CDCl₃, 20 °C): δ 153.9, 153.6, 144.3, 143.6, 143.5, 141.8, 141.6, 140.3, 134.7, 134.3, 132.3, 131.7, 131.4, 131.4, 131.3, 130.7, 129.8, 128.8, 128.4, 127.7, 127.6, 126.6, 126.5, 126.5, 118.8, 111.7, 58.5, 0.0 ppm; HRMS (ESI): calcd. for C₅₀H₃₅N₃S: 709.2546 (M+H)⁺, found 709.2542.

Supplementary data

Electronic supplementary information (ESI) available: Experimental procedures, NMR spectra, UV-vis spectra, mechanochromic effect, and computational data.

Acknowledgments

We acknowledge the support by DST, and CSIR Govt. of India, New Delhi. T J thanks UGC, B D thanks to CSIR New Delhi for their fellowships.

References

- 1 (a) Z. Chi, X. Zhang, B. Xu, X. Zhou, C. Ma, Y. Zhang, S. Liua and J. Xu, *Chem. Soc. Rev.*, 2012, **41**, 3878–3896; (b) Y. Sagara and T. Kato, *Nat. Chem.*, 2009, **1**, 605; (c) D. A. Davis, A. Hamilton, J. L. Yang, L. D. Cremar, D. Van Gough, S. L. Potisek, M. T. Ong, P. V. Braun, T. J. Martinez, S. R. White, J. S. Moore and N. R. Sottos, *Nature*, 2009, **459**, 68; (d) Y. J. Dong, B. Xu, J. B. Zhang, X. Tan, L. J. Wang, J. L. Chen, H. G. Lv, S. P. Wen, B. Li, L. Ye, B. Zou and W. J. Tian, *Angew. Chem. Int. Ed.*, 2012, **51**, 10782; (e) X. L. Luo, J. N. Li, C. H. Li, L. P. Heng, Y. Q. Dong, Z. P. Liu, Z. S. Bo and B. Z. Tang, *Adv. Mater.*, 2011, **23**, 3261.
- 2 M. S. Kwon, J. Gierschner, S. J. Yoon and S. Y. Park, *Adv. Mater.*, 2012, **24**, 5487.
- 3 (a) J. B. Birks, *Photophysics of Aromatic Molecules*, Wiley, London, U.K., 1970; (b) S. Jayanty and T. P. Radhakrishnan, *Chem.–Eur. J.*, 2004, **10**, 791; (c) H. J. Tracy, J. L. Mullin, W. T. Klooster, J. A. Martin, J. Haug, S. Wallace, I. Rudloe and K. Watts, *Inorg. Chem.*, 2005, **44**, 2003.
- 4 J. D. Luo, Z. L. Xie, J. W. Y. Lam, L. Cheng, H. Y. Chen, C. F. Qiu, H. S. Kwok, X. W. Zhan, Y. Q. Liu, D. B. Zhu and B. Z. Tang, *Chem. Commun.*, 2001, 1740. (b) Y. Li, T. Liu,

- H. Liu, M. Z. Tian, and Y. Li, *Acc. Chem. Res.*, 2014, **47**, 1186; (c) H. Liu, J. Xu, and Y. Li, *Acc. Chem. Res.*, 2010, **43**, 1496–1508; (d) Y. Hong, J. W. Y. Lam, and B. Z. Tang, *Chem. Soc. Rev.* 2011, **40**, 5361.
- 5 (a) Y. Dong, J. W. Y. Lam, A. Qin, J. Liu, Z. Li, B. Z. Tang, J. Sun and H. S. Kwok, *Appl. Phys. Lett.*, 2007, **91**, 011111; (b) J. Huang, X. Yang, J. Wang, C. Zhong, L. Wang, J. Qin and Z. Li, *J. Mater. Chem.*, 2012, **22**, 2478; (c) N. Zhao, Z. Y. Yang, J. W. Y. Lam, H. H. Y. Sung, N. Xie, S. J. Chen, H. M. Su, M. Gao, I. D. Williams, K. S. Wong and B. Z. Tang, *Chem. Commun.*, 2012, **48**, 8637; (d) J. Wang, J. Mei, R. Hu, J. Z. Sun, A. Qin and B. Z. Tang, *J. Am. Chem. Soc.*, 2012, **134**, 9956; (e) N. Zhao, M. Li, Y. L. Yan, J. W. Y. Lam, Y. L. Zhang, Y. S. Zhao, K. S. Wong and B. Z. Tang, *J. Mater. Chem. C*, 2013, **1**, 4640; (f) B. Xu, M. Xie, J. He, B. Xu, Z. Chi, W. Tian, L. Jiang, F. Zhao, S. Liu, Y. Zhang, Z. Xu and J. Xu, *Chem. Commun.*, 2013, **49**, 273; (g) B. Xu, Z. Chi, X. Zhang, H. Li, C. Chen, S. Liu, Y. Zhang and J. Xu, *Chem. Commun.*, 2011, **47**, 11080; (h) Y. Lin, G. Chen, L. Zhao, W. Z. Yuan, Y. Zhang, and B. Z. Tang, *J. Mater. Chem. C.*, 2015, **3**, 112–120; (i) X. Y. Shen, Y. J. Wang, E. Zhao, W. Z. Yuan, Y. Liu, P. Lu, A. Qin, Y. Ma, J. Z. Sun and B. Z. Tang, *J. Phys. Chem. C*, 2013, **117**, 7334–7347.
- 6 (a) S. Chen, Y. Li, W. Yang, N. Chen, H. Liu and Y. Li, *J. Phys. Chem. C*, 2010, **114**, 15109–15115; (b) H. Sakurai, M. T. S. Ritonga, H. Shibatani, T. Hirao, *J. Org. Chem.* 2005, **70**, 2754–2762; (c) A. Dhanabalan, J. K. J. van Duren, P. A. van Hal, J. L. J. van Dongen, R. A. Janssen, *J. Adv. Funct. Mater.* 2001, **11**, 255–262; (d) M. Zhang, H. N. Tsao, W. Pisula, C. Yang, A. K. Mishra, K. Müllen, *J. Am. Chem. Soc.* 2007, **129**, 3472–3473; (e) C. J. Shi, Y. Yao, Y. Yang, Q. B. Pei, *J. Am. Chem. Soc.* 2006, **128**, 8980–8986; (f) Q. Hou, Q. M. Zhou, Y. Zhang, W. Yang, R. Q. Yang, Y. Cao, *Macromolecules* 2004, **37**, 6299–6305; (g) Z. Zhu,

- D. Waller, R. Gaudiana, M. Morana, D. Muhlbacher, M. Scharber, C. Brabec, *Macromolecules* 2007, **40**, 1981–1986; (h) K. R. J. Thomas, J. T. Lin, M. Velusamy, Y. T. Tao, C. H. Chuen, *Adv. Funct. Mater.* 2004, **14**, 83–90.
- 7 (a) C. Dou, D. Chen, J. Iqbal, Y. Yuan, H. Zhang and Y. Wang, *Langmuir*, 2011, **27**, 6323–6329; (b) X. Zhang, Z. Ma, Y. Yang, X. Zhang, X. Jia and Y. Wei, *J. Mater. Chem. C*, 2014, **2**, 8932–8938.
- 8 (a) S. Li, Y. Shang, E. Zhao, Ryan. T. K. Kwok, J. W. Y. Lam, Y. Song and B. Z. Tang, *J. Mater. Chem. C*, 2015, **3**, 3445–3451; (b) H. Li, Z. Chi, X. Zhang, B. Xu, S. Liu, Y. Zhang and J. Xu, *Chem. Commun.*, 2011, **47**, 11273; (c) Z. Zhao, C. Deng, S. Chen, J. W. Y. Lam, W. Qin, P. Lu, Z. Wang, H. S. Kwok, Y. Ma, H. Qiu and B. Z. Tang, *Chem. Commun.*, 2011, **47**, 8847.
- 9 (a) R. Misra, T. Jadhav, B. Dhokale and S. M. Mobin, *Chem. Commun.*, 2014, **50**, 9076–9078; (b) T. Jadhav, B. Dhokale, S. M. Mobin and R. Misra, *RSC Adv.*, 2015, **5**, 29878–29884.
- 10 (a) R. Misra, P. Gautam, T. Jadhav and S. M. Mobin, *J. Org. Chem.*, 2013, **78**, 4940–4948; (b) R. Misra, P. Gautam and S. M. Mobin, *J. Org. Chem.*, 2013, **78**, 12440–12452
- 11 P. Gautam, R. Maragani, S. M. Mobin and R. Misra, *RSC Adv.*, 2014, **4**, 52526.
- 12 (a) Y. P. Li, F. Li, H. Y. Zhang, Z. Q. Xie, W. J. Xie, H. Xu, B. Li, F. Z. Shen, L. Ye, M. Hanif, D. G. Ma, and Y. G. Ma, *Chem. Commun.* **2007**, 231–233; (b) X. Y. Shen, W. Z. Yuan, Y. Liu, Q. Zhao, P. Lu, Y. Ma, I. D. Williams, A. Qin, J. Z. Sun and B. Z. Tang, *J. Phys. Chem. C*, 2012, **116**, 10541–10547.
- 13 G. F. Zhang, M. P. Aldred, W. L. Gong, C. Li and M. Q. Zhu, *Chem. Commun.*, 2012, **48**, 7711–7713.

TOC

